IEEE Photonics Journal
An IEEE Photonics Society Publication

Open Access

A High-Speed Second-Order Photonic Differentiator Based on Two-Stage Silicon Self-Coupled Optical Waveguide

Volume 6, Number 2, April 2014

Liang Zhang
Jiayang Wu
Xi Yin
Xiaowen Sun
Pan Cao
Xinhong Jiang
Yikai Su, Senior Member, IEEE

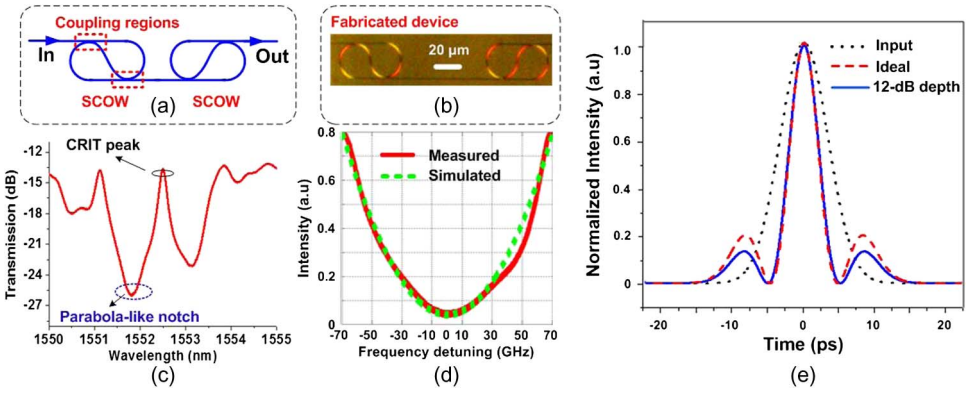

DOI: 10.1109/JPHOT.2014.2302806
1943-0655

A High-Speed Second-Order Photonic Differentiator Based on Two-Stage Silicon Self-Coupled Optical Waveguide

Liang Zhang, Jiayang Wu, Xi Yin, Xiaowen Sun, Pan Cao, Xinhong Jiang, and Yikai Su, *Senior Member, IEEE*

State Key Laboratory of Advanced Optical Communication Systems and Networks, Department of Electronic Engineering, Shanghai Jiao Tong University, Shanghai 200240, China

DOI: 10.1109/JPHOT.2014.2302806

Manuscript received January 10, 2014; accepted January 16, 2014. Date of publication January 29, 2014; date of current version March 3, 2014. This work was supported in part by the National Natural Science Foundation of China under Grant 61125504 and in part by the 863 High-Tech Program under Grant 2013AA013402. Corresponding author: Y. Su (e-mail: yikaisu@sjtu.edu.cn).

Abstract: In this paper, we propose and demonstrate an all-optical second-order differentiator based on a two-stage self-coupled optical waveguide on a silicon-on-insulator platform. The transmission spectrum of the fabricated device has a parabola-like filtering notch with a 3-dB bandwidth of up to ~100 GHz and a depth of ~12 dB. Experiments are carried out for 10-, 20-, and 40-Gb/s optical time-domain multiplexing (OTDM) picosecond pulse trains, and the second-order differentiations are achieved using the fabricated device.

Index Terms: High speed, second-order differentiator, silicon, two-stage self-coupled optical waveguide (TS-SCOW).

1. Introduction

The implementations of all-optical circuits for computing, signal processing, and networking could break the intrinsic speed limitation of electronics-based systems [1], [2]. The design of photonic equivalents of basic building blocks in electronic circuits is a primary step towards practical realization of all-optical circuits. Among them, temporal differentiator is an important component, which has a wide range of applications including ultrafast all-optical information processing and computing, optical pulse shaping and coding, ultra-wideband (UWB) microwave signal generation, and direct phase reconstruction of arbitrary optical signals [3], [4]. In Refs. [5]–[7], first-order differentiators were studied using various methods. On the other hand, high-order differentiator is also of significant interest for many applications, such as reconfigurable UWB pulse shaping, high-order Hermite–Gaussian waveforms and high-order differential-equation solver [8], [9]. References [10], [11] have demonstrated high-order differentiators based on fiber-optics technologies or bulky systems. In Ref. [12], an integrated silicon-based high-order temporal differentiator was realized using cascaded micro-ring resonators (MRRs). However, the 3-dB bandwidth of the resonance notch was ~15 GHz, with a processing speed of 5-Gb/s.

In this work, we fabricate a device on a silicon-on-insulator (SOI) platform with a structure of two-stage self-coupled-optical-waveguide (TS-SCOW) [13]. The transmission spectrum of the fabricated device has a parabola-like resonance notch with a 3-dB bandwidth of up to ~100-GHz, which can be used as high-speed second-order differentiator. Experiments are carried out for 10-Gb/s, 20-Gb/s

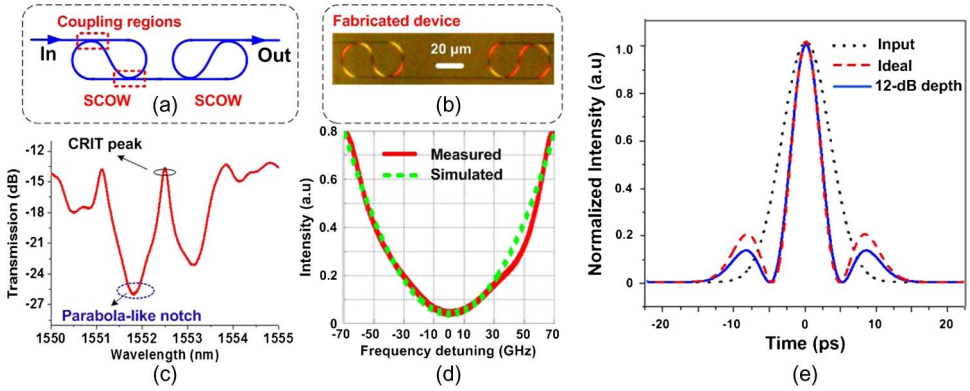

Fig. 1. (a) Schematic diagram of the proposed TS-SCOW; (b) micrograph of the fabricated device; (c) measured transmission spectrum of the TS-SCOW; (d) zoom-in view of the parabola-like resonance notch marked with blue dashed line in (c); (e) inputted Gaussian pulse (black dot line) and simulation results of the ideal second-order differentiation (red dash line) and the second-order differentiation using 12-dB depth notch (blue solid line).

and 40-Gb/s optical time domain multiplexing (OTDM) pico-second pulse signals and the second-order differentiations are successfully obtained. To the best of our knowledge, it is the most compact second-order photonic differentiator implemented by an on-chip silicon device with a record processing speed of up to 40 Gb/s.

2. Device Fabrication and Analysis

The configuration of the TS-SCOW is shown in Fig. 1(a). It consists of two cascaded SCOWs connected by a central waveguide. For each SCOW, coupled-resonator-induced-transparency (CRIT) can be achieved based on mutual coupling between the clockwise (CW) and counterclockwise (CCW) degenerate resonance modes [13]. When there is weak coupling in the coupling regions shown in Fig. 1(a), one can obtain a CRIT peak with parabola-like notches on both sides in the transmission spectrum depicted in Fig. 1(c). According to Ref. [13], the SCOW is generally equivalent to a two-stage micro-ring resonators (MRR). However, compared with cascaded MRRs [12], precise alignment of the resonance wavelength is not necessary for a SCOW resonator, since the SCOW resonator itself can co-excite two degenerate resonance modes in one cavity with a same resonance wavelength [13]. Here, a structure with two cascaded SCOWs is chosen to further increase the bandwidth and depth of the parabola-like resonance notch, thus it is more suitable to perform as a high-speed second-order differentiator.

The designed device was fabricated on a SOI wafer with a 220-nm top silicon layer and a 2-μm-thick buried oxide layer. A micrograph of the fabricated device is depicted in Fig. 1(b). The cross-sectional dimension of the waveguides is 450 nm $\times$ 220 nm. The gap size in the coupling regions is 180 nm and the straight coupling length in the coupling regions is very short to achieve a relatively weak coupling. The layout is defined by 248-nm deep ultraviolet (DUV) photolithography followed by inductively coupled plasma (ICP) etching. It is assumed that the waveguide group index of the transverse electric (TE) mode is $n_g = 4.33$ and the propagation loss factor is $\alpha = \sim$4.5 dB/cm. In order to couple light in and out of the chip with single mode fibers, grating couplers for TE polarization are fabricated at both ends.

The measured spectrum of the fabricated device is shown in Fig. 1(c), CRIT peak and parabola-like notches are observed. Zoom-in view of the parabola-like notch is illustrated in Fig. 1(d) using the red solid curve, which approximates to the ideal parabola curve shown by the green dashed line. The 3-dB bandwidth and the notch depth of the measured parabola-like notch are $\sim$100 GHz and $\sim$12 dB, respectively, which can be used for experimental demonstration of high-speed second-order differentiation. In order to investigate the influence of the notch depth, we perform simulations and the results are shown in Fig. 1(e). When an ideal Gaussian pulse (black dot line) is used as an

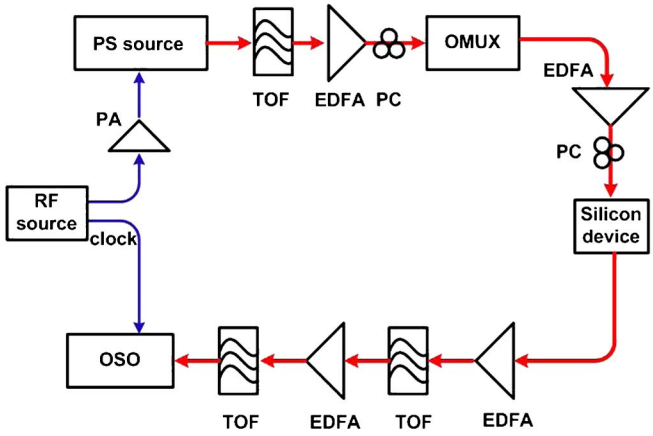

Fig. 2. Experimental setup of the all-optical second-order differentiator based on the silicon TS-SCOW. RF: radio frequency, PS: pico-second, EA: electrical amplifier, TOF: tunable optical filter, OSO: optical sampling oscilloscope.

input signal, a second-order differentiation pulse (blue line) can be achieved with the 12-dB depth notch of the fabricated device. Compared with the ideal second-order differentiation pulse (red dash line), small deviations of the side-lobes are observed for the 12-dB depth notch. There are two methods to improve the notch depth: 1) to balance the coupling strength in the coupling region and the propagation loss in the SCOW so the device approximates critical coupling; 2) to design a device with more cascaded SCOWs.

3. Experimental Setup and Results

An experiment is carried out to test the performance of the fabricated silicon TS-SCOW as a second-order photonic differentiator for the pico-second pulse trains. The experimental setup is depicted in Fig. 2. A 10-GHz radio frequency (RF) clock from a pulse pattern generator (PPG ANRITSE MP1763C) is amplified and used as an electrical driver for a pico-second pulse generator (u2t TMLL 1550), working in active mode-locking state. The output of the TMLL 1550 is a pico-second pulse train with a repetition frequency of 10 GHz, whose spectrum is shown in Fig. 3(a). The temporal waveform is provided in Fig. 3(b) with a full width half maximum (FWHM) of 2.8 ps, which is observed by a 500-GHz optical sampling oscilloscope (OSO Alnair Lab EYE-2000C). In order to match the bandwidth of the silicon TS-SCOW and reduce the influence of the device's sideband spectrum, a following tunable optical filter (TOF) is utilized to pre-shape the pico-second pulse train. The spectrum after the TOF is provided in Fig. 3(c) and the temporal waveform is shown in Fig. 3(d), whose FWHM is broadened to 6.2 ps. Afterwards, an erbium-doped fiber amplifier (EDFA) is used to boost the optical power to 15 dBm and an optical multiplexer (OMUX) is employed to generate 10-Gb/s, 20-Gb/s and 40-Gb/s OTDM signals. After amplification, the OTDM signal is fed into the silicon TS-SCOW by a vertical coupling system. A polarization controller (PC) is inserted before the silicon device to make sure that the input light is transverse electrical (TE) polarized. The output signal after the TS-SCOW is amplified by another two EDFAs to compensate the ~13 dB power loss induced by the vertical coupling system and the ~12 dB notch filtering loss caused by the silicon device. The optical spectrum and temporal waveform after the TS-SCOW are shown in Fig. 3(e) and (f), respectively. Fig. 4 demonstrates the experimental and simulation results of the 10-Gb/s, 20-Gb/s and 40-Gb/s OTDM signals before and after the second-order differentiations. The original 10-Gb/s, 20-Gb/s and 40-Gb/s signals are shown in insets (i) of Fig. 4(a)–(c), respectively. The shape discrepancies among the pulses of the 20-Gb/s and 40-Gb/s OTDM signals are mainly caused by the imperfect attenuations and time delays in the multiple-stage propagation paths within the OMUX. Insets (ii) of Fig. 4(a)–(c) illustrate the experimental results of the second-order differentiations for the 10-Gb/s, 20-Gb/s and 40-Gb/s OTDM signals, which agree with the simulation

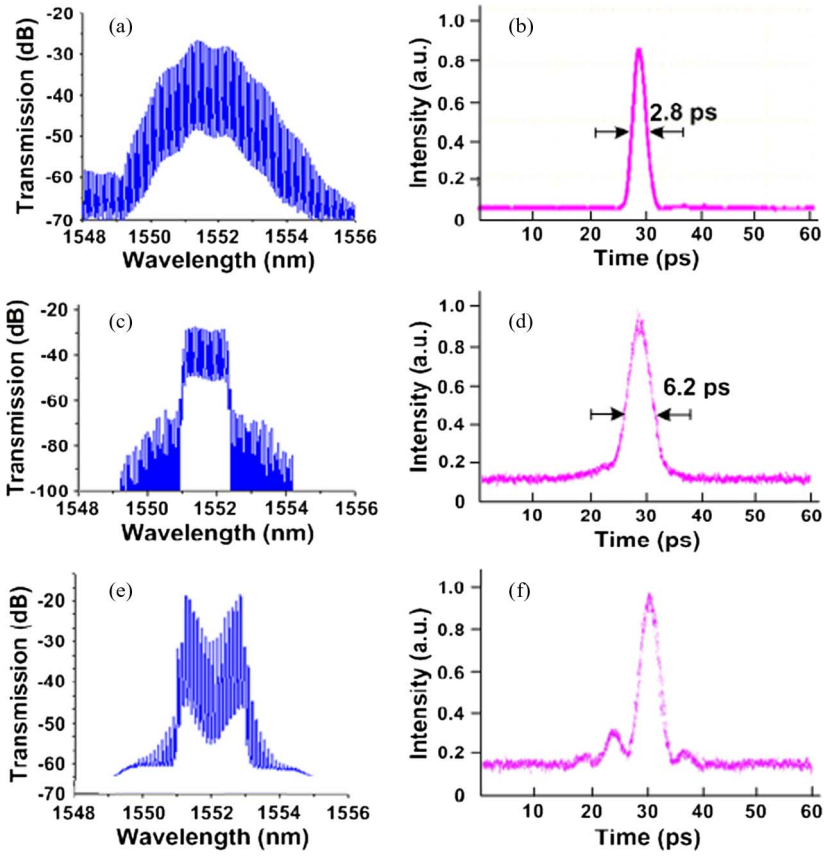

Fig. 3. (a) and (b) Optical spectrum and temporal waveform of the pico-second pulse, respectively. (c) and (d). Spectrum and temporal waveform after the pre-shape TOF, respectively. (e) and (f) Optical.

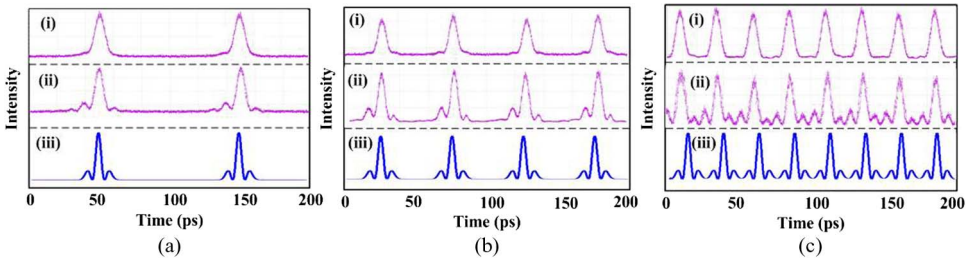

Fig. 4. (a-i), (b-i), and (c-i). Original 10-Gb/s, 20-Gb/s, and 40-Gb/s OTDM pulses, respectively. (a-ii), (b-ii), and (c-ii). Experimental observations of the second-order differentiations of the 10-Gb/s, 20-Gb/s, and 40-Gb/s OTDM pulses, respectively. (a-iii), (b-iii). and (c-iii). Simulation.

results, as shown in insets (iii) of Fig. 4. It is noted that the TS-SCOW with the 100-GHz bandwidth can operate for a signal above 40-Gb/s. In the experiment, however, the non-ideal pulses with certain pedestals of the OTDM signal limit higher speed operation at 80 Gb/s. In our experiment, since the waveforms captured by the 500-GHz OSO (Alnair 2000C) are in jpg format, the accuracy of the second-order differentiation is not qualitatively analyzed, but expected to be ~10% in comparison with [12]. Theoretically, the second-order differentiated results of Gaussian pulses are even-symmetry Hermite–Gaussian pulses (insets (iii) in Fig. 4). Here, the deviations of the two side-lobes

of the experimental results can be attributed to two main reasons: 1) the imperfect parabola curve of the notch profile, which may induce fraction-order differentiations [10]; 2) the limited 3-dB bandwidth of the parabola-like notch at the resonance wavelength [12], [14].

4. Conclusion

We have fabricated a two-stage silicon SCOW, and a parabola-like filtering notch is observed with a 3-dB bandwidth of ~100 GHz and a depth of ~12 dB. The fabricated device is used as an all-optical second-order differentiator. Experiments are performed for the 10-Gb/s, 20-Gb/s and 40-Gb/s OTDM pico-second pulse trains. The second-order differentiations are achieved and the experimental results agree with the simulation ones. The proposed second-order all-optical differentiator could be a competitive candidate for high-speed silicon-based integrated photonics components.

References

[1] M. Li, D. Janner, J. Yao, and V. Pruneri, "Arbitrary-order all-fiber temporal differentiator based on a fiber Bragg grating: Design and experimental demonstration," *Opt. Exp.*, vol. 17, no. 22, pp. 19798–19807, Oct. 2009.
[2] J. Azana, R. Slavik, Y. Park, and M. Kulishov, "Ultrafast analog all-optical signal processors based on fiber-grating devices," *IEEE Photon. J.*, vol. 2, no. 3, pp. 359–386, Jun. 2010.
[3] R. Slavik, Y. Park, M. Kulishov, and J. Azana, "Terahertz-bandwidth high-order temporal differentiators based on phase-shifted long-period fiber gratings," *Opt. Lett.*, vol. 34, no. 20, pp. 3116–3118, Oct. 2009.
[4] M. Kulishov and J. Azana, "Long-period fiber gratings as ultrafast optical differentiators," *Opt. Lett.*, vol. 30, no. 20, pp. 2700–2702, Oct. 2005.
[5] J. Xu, X. Zhang, J. Dong, D. Liu, and D. Huang, "High speed all optical differentiator based on semiconductor optical amplifier and optical filter," *Opt. Lett.*, vol. 32, no. 13, pp. 1872–1874, Jul. 2007.
[6] R. Slavik, Y. Park, M. Kulishov, and J. Azana, "Stable all-fiber photonic temporal differentiator using a long-period fiber grating interferometer," *Opt. Commun.*, vol. 282, no. 12, pp. 2339–2342, Jun. 2009.
[7] F. Liu, T. Wang, M. Qiu, and Y. Su, "Compact optical temporal differentiator based on silicon microring resonator," *Opt. Exp.*, vol. 16, no. 20, pp. 15880–15886, Sep. 2008.
[8] J. Capmany, B. Ortega, and D. Pastor, "A tutorial on microwave photonic filters," *IEEE/OSA J. Lightw. Technol.*, vol. 24, no. 1, pp. 201–229, Jan. 2006.
[9] H. Shahoei, J. Albert, and J. Yao, "Tunable fractional order temporal differentiator by optically pumping a tilted fiber Bragg grating," *IEEE Photon. Technol. Lett.*, vol. 24, no. 9, pp. 730–732, May 2012.
[10] M. Li, L. Shao, J. Albert, and J. Yao, "Continuously tunable photonic fractional temporal differentiator based on a tilted fiber Bragg grating," *IEEE Photon. Technol. Lett.*, vol. 23, no. 4, pp. 251–253, Feb. 2011.
[11] N. Q. Ngo, S. F. Yu, S. C. Tin, and C. H. Kam, "A new theoretical basis of higher-derivative optical differentiators," *Opt. Commun.*, vol. 230, no. 1-3, pp. 115–129, Jan. 2004.
[12] J. Dong, A. Zheng, D. Gao, and X. Zhang, "High-order photonic differentiator employing on-chip cascaded microring resonators," *Opt. Lett.*, vol. 38, no. 5, pp. 628–630, Mar. 2013.
[13] L. Zhou, T. Ye, and J. Chen, "Coherent interference induced transparency in self-coupled optical waveguide-based resonators," *Opt. Lett.*, vol. 36, no. 1, pp. 13–15, Jan. 2011.
[14] Y. Hu, L. Zhang, Y. Su, and J. Yu, "An ultra-high-speed photonic temporal differentiator using cascaded SOI microring resonators," *J. Opt.*, vol. 14, no. 6, pp. 065501–065508, May 2012.